Supporting Information

Assembly of copper-cluster into framework: enhancing structural stability and photocatalytic HER performance

Yue Xu,[‡a] Qing-Guo Dong,[‡a] Jian-Peng Dong,[a] Huan Zhang,[a] Bo Li,*[b] Rui Wang*[a] and Shuang-Quan Zang*[a]

[a] Henan Key Laboratory of Crystalline Molecular Functional Materials, Henan International Joint Laboratory of Tumor Theranostical Cluster Materials, Green Catalysis Center, and College of Chemistry, Zhengzhou University, Zhengzhou 450001, China

[b] Collaborative Innovation Center of Water Security for Water Source Region of Mid-line of South-to-North Diversion Project of Henan Province, College of Chemistry and Pharmacy Engineering, Nanyang Normal University, Nanyang 473061, China

E-mail: zangsqzg@zzu.edu.cn; wangruijy@zzu.edu.cn; libony0107@nynu.edu.cn

Experimental Details

Materials and reagents. All of the ingredients for the synthesis were purchased commercially and utilized without further purification.

Instrumentation. Powder X-ray powder diffraction (PXRD) patterns were recorded by using a Rigaku D/Max-2500PC diffractometer with Cu Kα1 radiation (λ = 1.540598 Å) at room temperature. TG analyses of the compounds were performed on a TGA-Q50 thermal analyzer from room temperature to 600 °C at a heating rate of 10 °C/min under an N_2 atmosphere. Fourier transform infrared (FT-IR) spectra were recorded on a Bruker TENSOR 27 FT-IR spectrometer in the 400-4000 cm^{-1} region. Elemental analyses (EA) were carried out with a Perkin-Elmer 240 elemental analyzer. UV-visible absorption spectra were recorded on a UH4150 spectrophotometer. The Ultraviolet Photoelectron Spectrometer (UPS) was recorded using a PHI5000 VersaProbe III spectrophotometer with a 21.2 eV photon energy He I light source. The adsorption isotherms of N_2 were measured by a volumetric method automatic volumetric adsorption equipment (Belsorp Max) at 77 K.

Crystallographic data collection and structural refinement. SCXRD measurements of Cu_8SN_4 and Cu_6-Cu-MOF were performed at 200 K on a Rigaku XtaLAB Pro diffractometer with Cu-Kα radiation (λ = 1.54184 Å). Data collection and reduction were performed using the program CrysAlisPro. All the structures were solved with direct methods (SHELXS)[1] and refined by full-matrix least-squares on F^2 using OLEX2, [2] which utilizes the SHELXL-2015 module.[3] The imposed restraints and constraints (ISOR, DFIX, DELU, TRIA, etc.) in the least-squares refinement of each structure were commented in the corresponding crystallographic CIF files. The crystal structures are visualized by DIAMOND3.2. Detailed information about the X-ray crystallography data, intensity collection procedure, and refinement results for all cluster compounds are summarized in Tables S1 and S2.

Synthesis

Synthesis of Cu_8SN_4. (^{t}BuSCu)$_n$ (0.008 g,0.052 mmol) are added to methylbenzene (2.0 ml) and 20 μL trifluoroacetic acid is added during the stirring process, and then mixed with 2 mL of Tetrahydrofuran containing 4-(4-Pyridinyl)thiazole-2-thiol (0.005 g, 0.026 mmol) under stirring and subsequently filtered. The filtrate was slowly evaporated at room temperature, and a large number of yellow block crystals were obtained after 6h (yield is 75% based on Cu).

Synthesis of $Cu_2I_2(3\text{-pc})_4$ (3-pc = 3-Picoline). The synthesis of $Cu_2I_2(3\text{-pc})_4$ was carried out by a modified version of the reported method.[4] CuI (0.19 g, 1.0 mmol) was first well-dispersed in 10 mL acetone in an open reaction vial, and 3-pc (0.37 g, 4.0 mmol) was slowly added under magnetic stirring at room temperature. The pure phase of the sample was collected by filtration after 10 min of continuous stirring (yield is 83% based on Cu). This compound was used as the precursor and was remade in large quantities for the synthesis of other structures.

Synthesis of CCMOF. 0.0135 mg Cu_8SN_4 was added into 2 mL DMF and dissolved by ultrasound. 0.0075 mg $Cu_2I_2(3\text{-pc})_4$ was added to 3 mL acetone and dissolved by ultrasound. DMF solution of Cu_8SN_4 was added to acetone solution of $Cu_2I_2(3\text{-pc})_4$ in the course of stirring, then stirred for 1~2 minutes, the filtrate evaporated and crystallized at room temperature, and green bulk Cu_6-Cu-MOF was obtained after 2 days (yield is 32% based on Cu).

Photocatalytic HER Experiments. The photocatalytic HER reaction was carried in a 60 mL Pyrex cell with visible light. In a typical photocatalytic experiment, the catalyst (2.0 mg) was suspended in H_2O/EtOH (v:v = 1:1) containing TEA (3 mL) and fluorescein (9.0 mg). Before irradiation, the suspension of the catalyst was dispersed in an ultrasonic bath for 10 minutes, and then N_2 was bubbled through the reaction mixture

for 20 minutes to completely remove oxygen. Sampling was conducted intermittently through the silicone rubber septum during experiments. The amount of produced H_2 was monitored in real-time by GC analysis of the headspace gases by using an Agilent GC7820 Gas Chromatograph (N_2 as the gas carrier).

Electrochemical measurements. Take two milligrams of samples (CCMOF), add 0.5 ml of ethanol and 10 μL of Nafion soulution, respectively, and ultrasonically disperse for 20 minutes. Take 30 μL of the dispersion and drop it onto the glassy carbon electrode to prepare a working electrode. The standard three-electrode system was used on the electrochemical workstation (CHI66E), the Ag/AgCl was used as the reference electrode, and 0.5 M sodium sulfate solution as the electrolyte. The EIS experiment was carried out with a starting potential of -0.4 V and a frequency range of 10^{6}−10^{-2} Hz.

Supplementary Figures S1-S19

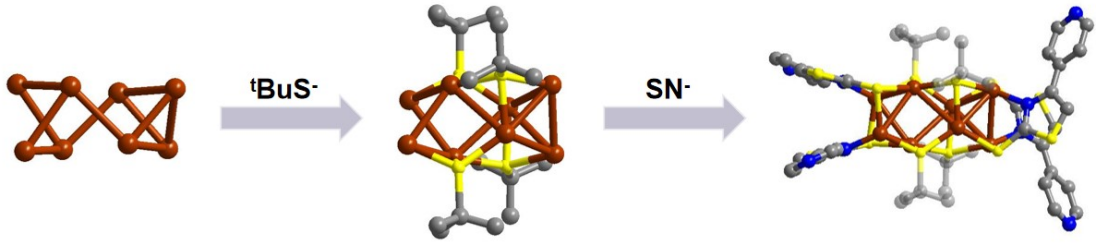

Figure S1. The structure and coordination mode of Cu_8SN_4 cluster unit.

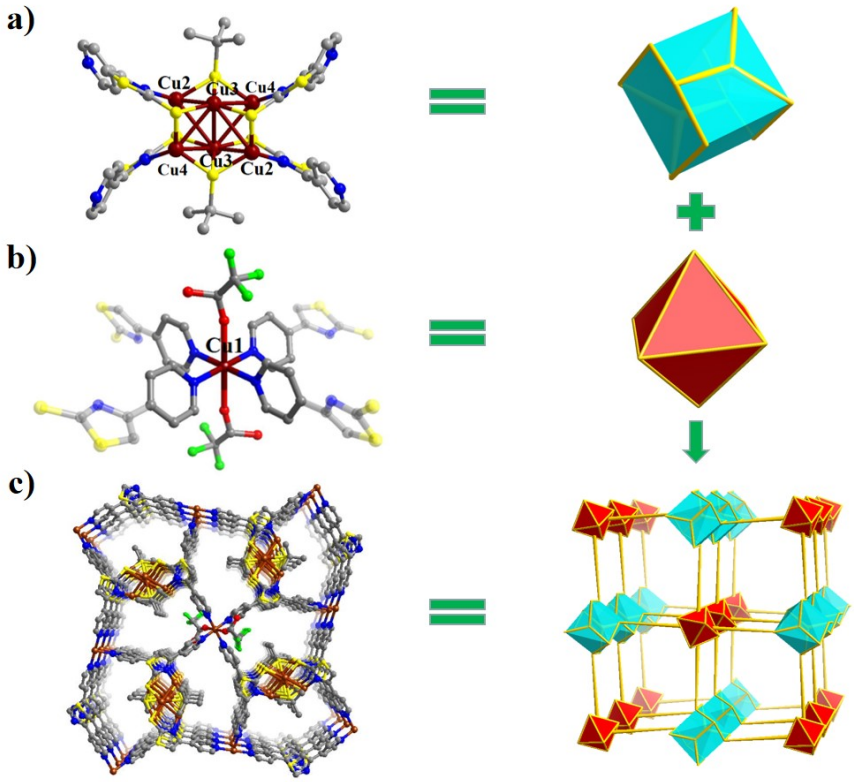

Figure S2. a) Hexanuclear $[Cu_6(^tBuS^-)_2(SN^-)_4]$ SBUs with distorted tetragonal bipyramidal geometry; b) Six-coordinated single-core copper node with octahedral configuration; c) CCMOF with 2-dimensional A-A stacking and its topological structure. (Color code: C, gray; Cu, brown; S, yellow; O, red; N，blue; F, bright green; H atoms are omitted for clarity.) The Cu_6 secondary building units (SBUs) presents an unusual twisted tetragonal bipyramidal geometry in which Cu2 and Cu4 atoms lie in the equatorial plane while two Cu3 atoms occupying parallel positions in the plane. Three S atoms from two distinct SN ligands and one tBuS- ligand coordinated Cu(I) at both ends of a twisted polyhedron, where the observed bond lengths of Cu-S were 2.219 ~ 2.349 Å. The copper cluster units were interconnected by Cu(II) center to develop a two-dimensional AA stacking system.

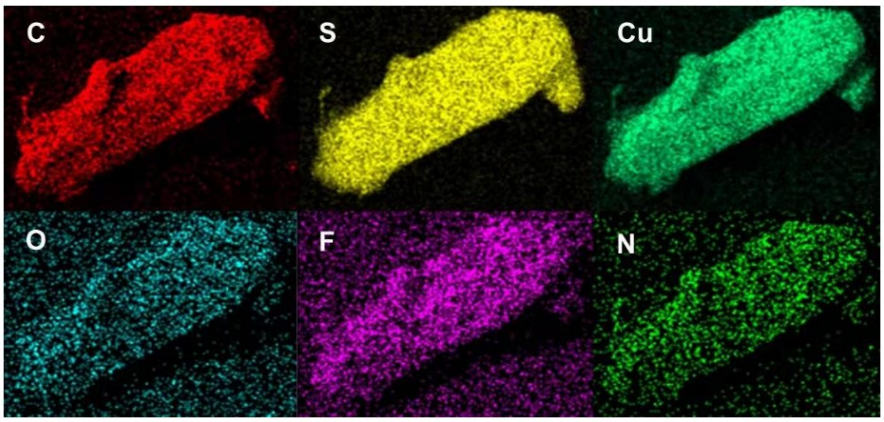

Figure S3. EDS elemental mapping images of CCMOF.

Table S1. X-ray measurements and structure solution of Cu_8SN_4.

	Cu_8SN_4
Empirical formula	$C_{48}H_{56}Cu_8N_8S_{12}$
Formula weight	1638.04
Temperature/K	199.99 (10)
Crystal system	Orthorhombic
Space group	$P2_12_12$
a / Å	10.1385(2)
b / Å	19.1450(5)
c / Å	15.7602(3)
α / °	90
β / °	90
γ / °	90
Volume / Å^3	3059.08(12)
Z	2
ρ_{calc} g / cm^3	1.778
μ / mm^{-1}	7.135
F (000)	1648.00
Crystal size / mm^3	0.3 × 0.1 × 0.1
Radiation	Cu Kα (λ = 1.54184)
2θ range for data collection/°	7.266 to 148.766
Index ranges	-7 ⩽ h ⩽ 12, -23 ⩽ k ⩽ 23, -19 ⩽ l ⩽ 18
Reflections collected	10734
Independent reflections	5537 [R_{int} = 0.0380, R_{sigma} = 0.0535]
Data / restraints / parameters	5537/51/379
Goodness-of-fit on F^2	1.059
Final R indexes [all data]	R_1 = 0.0449, wR_2 = 0.1138
Final R indexes [I >= 2σ (I)]	R_1 = 0.0525, wR_2 = 0.1189
Largest diff. peak/hole / e Å^{-3}	0.54/-0.54
Flack parameter	-0.02(2)
CCDC	2079381

$R_1 = \sum||F_o|-|F_c||/\sum|F_o|$. $wR_2 = [\sum w(F_o^2-F_c^2)^2/\sum w(F_o^2)^2]^{1/2}$

Table S2. X-ray measurements and structure solution of CCMOF.

	CCMOF
Empirical formula	$C_{56}H_{62}Cu_7F_6N_8O_8S_{10}$
Formula weight	1854.51
Temperature/K	200.00(10)
Crystal system	monoclinic
Space group	$P2_1/c$
a / Å	9.63270(10)
b / Å	19.2788(3)
c / Å	18.8668(2)
α / °	90
β / °	91.1760(10)
γ / °	90
Volume / Å^3	3502.96(8)
Z	2
ρ_{calc} g / cm^3	1.758
μ / mm^{-1}	5.702
F (000)	1870.0
Crystal size / mm^3	0.4 × 0.2 × 0.1
Radiation	Cu Kα (λ = 1.54184)
2θ range for data collection / °	6.556 to 148.078
Index ranges	$-9 \leqslant h \leqslant 11$, $-23 \leqslant k \leqslant 21$, $-19 \leqslant l \leqslant 23$
Reflections collected	20888
Independent reflections	6930 [R_{int} = 0.0454, R_{sigma} = 0.0532]
Data / restraints / parameters	6930/92/452
Goodness-of-fit on F^2	1.045
Final R indexes [I>=2σ (I)]	R_1 = 0.0645, wR_2 = 0.1758
Final R indexes [all data]	R_1 = 0.0829, wR_2= 0.1904
Largest diff. peak/hole / e Å^{-3}	1.45/-1.04
CCDC	2079399

$R_1 = \sum||F_o|-|F_c||/\sum|F_o|$. $wR_2 = [\sum w(F_o^2-F_c^2)^2/\sum w(F_o^2)^2]^{1/2}$

Table S3. Bond Lengths in Cu_8SN_4 at 200 K.

Cu4-Cu4[1]	2.890(2)	N2-C8	1.313(10)
Cu4-Cu3	2.8256(14)	N2-C6	1.371(9)
Cu4-N3[1]	2.7330(14)	C23-C24	1.372(11)
Cu4-S5[1]	2.268(2)	C23-C22	1.465(11)
Cu4-S4	2.225(2)	C23-C27	1.384(13)
Cu4-N3	2.044(5)	C9-C12	1.517(13)
Cu1-Cu2[1]	2.9256(16)	C9-C11	1.516(13)
Cu1-Cu2	2.6399(15)	C9-C10	1.506(12)
Cu1-S3	2.190(2)	C24-C25	1.361(13)
Cu1-S2[1]	2.274(3)	C22-C21	1.383(12)
Cu1-N2	2.011(6)	C27-C26	1.376(13)
Cu3-Cu2[1]	2.9903(14)	N4-C25	1.316(14)
Cu3-S5[1]	2.2790(19)	N4-C26	1.316(14)
Cu3-S41	2.286(2)	C4-C5	1.347(13)
Cu3-S3	2.2463(19)	C4-C3	1.369(16)
Cu2-S4	2.2594(19)	C5-C6	1.483(11)
Cu2-S3	2.331(2)	C5-C1	1.352(14)
Cu2-S2	2.2757(19)	C6-C7	1.344(11)
S5-C20	1.738(8)	N1-C3	1.336(16)
S4-C9	1.883(8)	N1-C2	1.276(17)
S3-C13	1.900(10)	C13-C15	1.54(2)

S2-C8	1.756(8)	C13-C19	1.55(2)
S1-C8	1.716(8)	C13-C17	1.41(2)
S1-C7	1.693(9)	C13-C18	1.61(3)
S6-C20	1.712(8)	C13-C14	1.42(3)
S6-C21	1.691(10)	C13-C16	1.67(3)
N3-C20	1.324(9)	C1-C2	1.431(17)
N3-C22	1.390(9)		

[1]-1*x*, 1-*y*, +*z*

Table S4. Bond Lengths in CCMOF at 200 K.

Cu4-N2	2.027(4)	N3-C9	1.337(8)
Cu4-N2[1]	2.027(4)	N1-C3	1.381(7)
Cu4-N3[1]	2.051(4)	N1-C1	1.315(7)
Cu4-N3	2.051(4)	C14-C11	1.472(7)
Cu4-O1	2.437(4)	C14-C15	1.350(10)
Cu3-O1[1]	2.437(4)	C11-C10	1.380(8)
Cu3-Cu1[2]	3.0245(11)	C11-C12	1.379(8)
Cu3-Cu2[2]	2.6731(11)	C6-C5	1.376(8)
Cu3-Cu2[3]	2.9097(11)	C4-C5	1.385(8)
Cu3-S1[2]	2.2472(16)	C4-C3	1.474(8)
Cu3-S5	2.2189(16)	C4-C8	1.378(8)
Cu3-N4	2.6537(4)	C3-C2	1.351(8)

Cu1-Cu2[4]	3.0301(12)	O3-C30	1.194(10)
Cu1-Cu2	2.6537(11)	C7-C8	1.368(9)
Cu1-S4[5]	2.2630(15)	C13-C12	1.387(8)
Cu1-S5[6]	2.2314(15)	C18-C19	1.534(11)
Cu1-N1	2.008(4)	C18-C17	1.492(11)
Cu2-Cu2[4]	2.9501(16)	C18-C20	1.500(11)
Cu2-S1	2.2865(15)	C10-C9	1.379(8)
Cu2-S4[6]	2.3042(16)	C21-C22	1.444(8)
Cu2-S5[6]	2.3494(15)	C21-O2	1.386(8)
S1-C1	1.744(6)	C30-C29	1.490(13)
S4-C16	1.742(6)	C30-C31	1.503(13)
S5-C18	1.874(7)	O4-C32	1.222(15)
S2-C1	1.713(5)	C32-C33	1.49(2)
S2-C2	1.709(6)	C32-C34	1.404(18)
S3-C16	1.709(6)	O1-C21	1.282(7)
S3-C15	1.701(8)	C22-F1	1.364(11)
N4-C14	1.375(7)	C22-F4	1.407(9)
N4-C16	1.323(6)	C22-F5	1.427(15)
N2-C6	1.339(8)	C22-F19	1.166(10)
N2-C7	1.328(8)	C22-F7	1.332(11)
N3-C13	1.329(8)	C22-F11	1.369(10)

[1]1-*x*,1-*y*, 1-*z*; [2]+*x*, 1/2-*y*, 1/2+*z*; [3]1-*x*, 1/2+*y*, 3/2-*z*; [4]1-*x*, -*y*, 1-*z*; [5]+*x*, 1/2-*y*, -1/2+*z*; [6]1-*x*, -1/2+*y*, 3/2-*z*

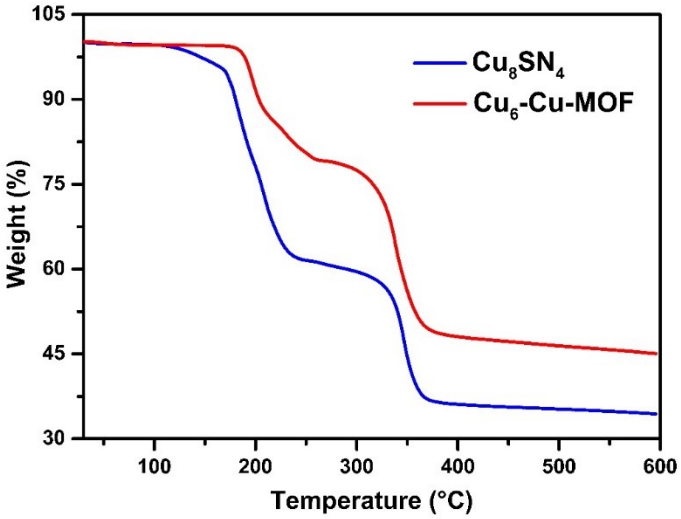

Figure S4. TGA plots of Cu_8SN_4 cluster and CCMOF under N_2 atmosphere.

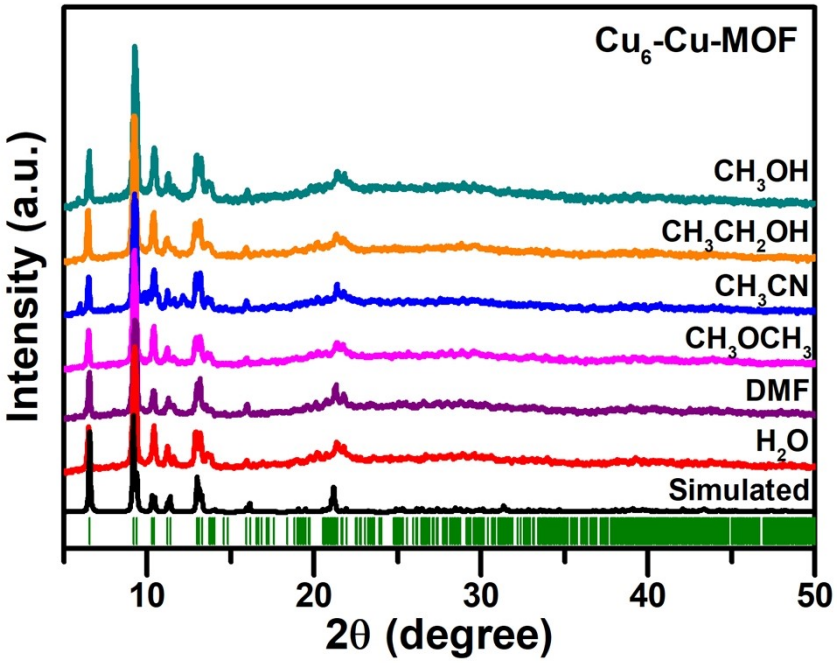

Figure S5. PXRD patterns of CCMOF immersed in different common organic solvents for 48 hours.

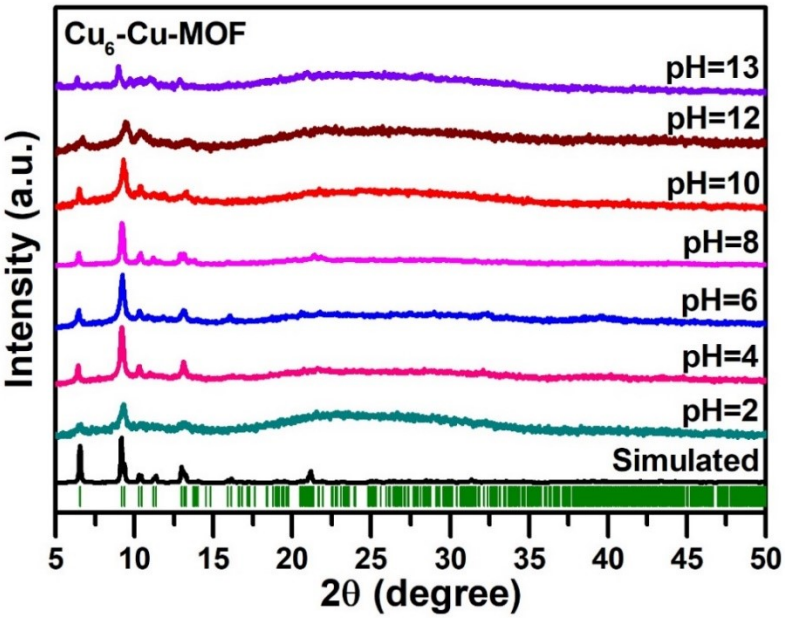

Figure S6. PXRD patterns of CCMOF treated with different pH for 24 hours.

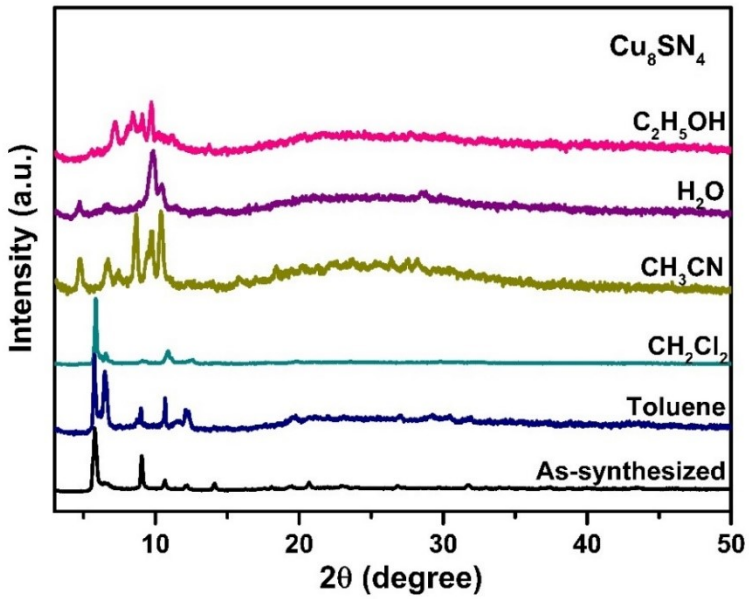

Figure S7. PXRD patterns of Cu_8SN_4 immersed in different common organic solvents for 24 hours.

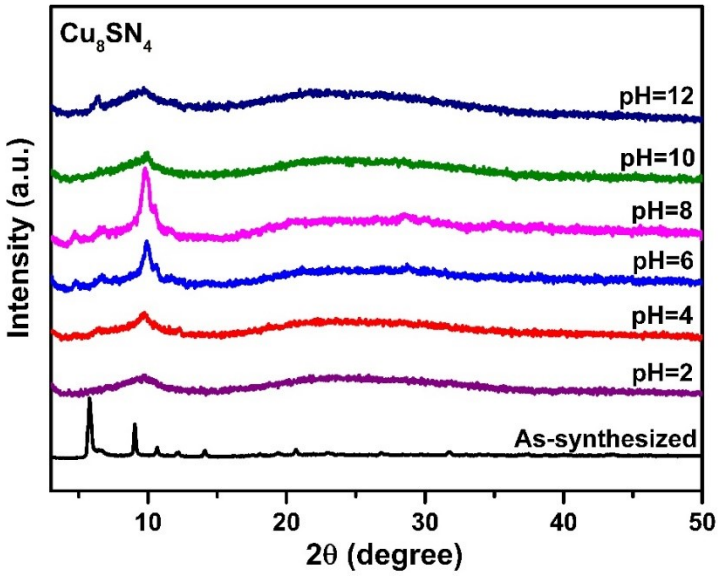

Figure S8. PXRD patterns of Cu_8SN4 treated with different pH for 24 hours.

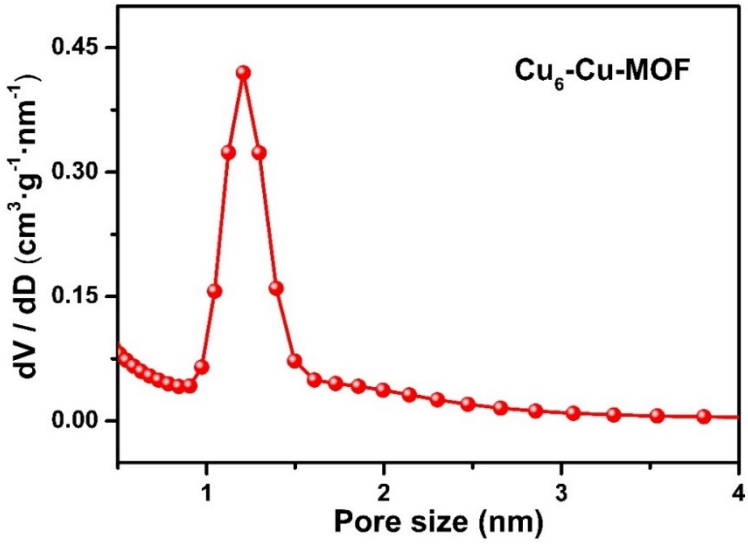

Figure S9. Pore size distribution profile of CCMOF based on nonlocal density function theory.

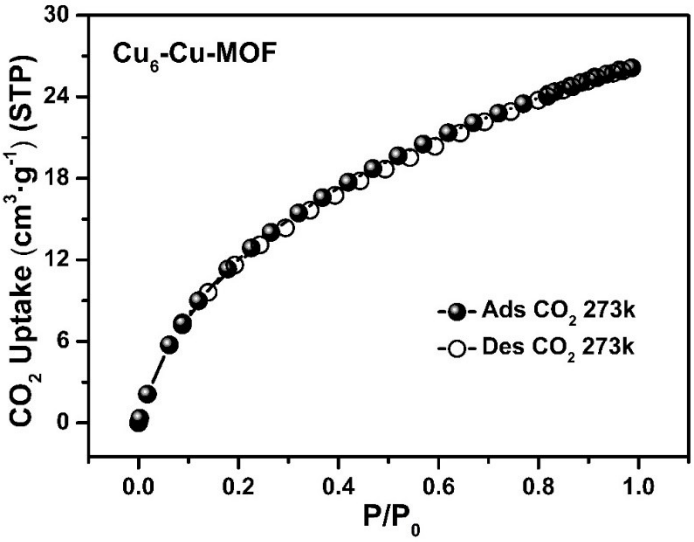

Figure S10. CO_2 sorption isotherms of CCMOF at 273 K.

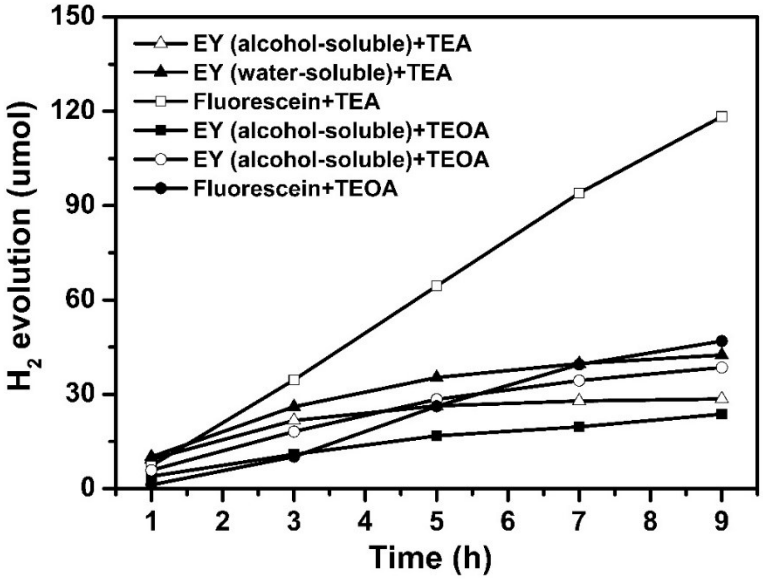

Figure S11. The effect of photosensitizer and sacrificial agent on H_2 evolution. H_2 evolution condition: MeOH/H_2O (1:1) in the presence of 2 mg of CCMOF in 30 mL solution containing sacrificial agent (3 mL) and 10 mg of photosensitizer under an inert atmosphere. The system was irradiated with visible light.

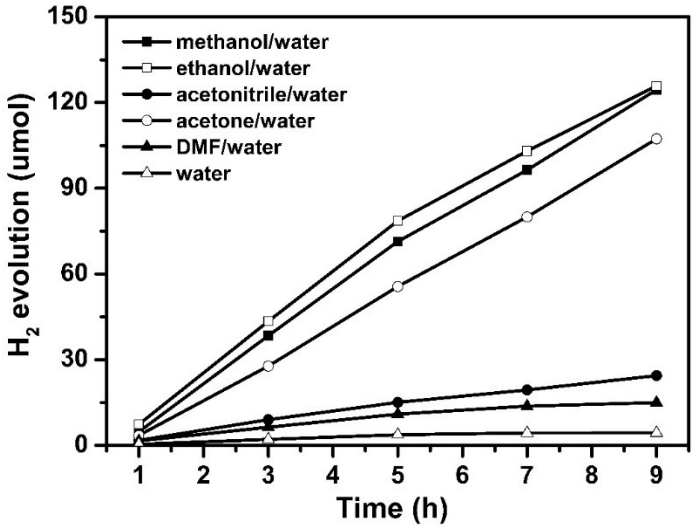

Figure S12. The effect of solvents on H_2 evolution. H_2 evolution condition: 2 mg of CCMOF in 30 mL solution containing TEA (3 mL) and 10 mg of fluorescein under an inert atmosphere. The system was irradiated with visible light.

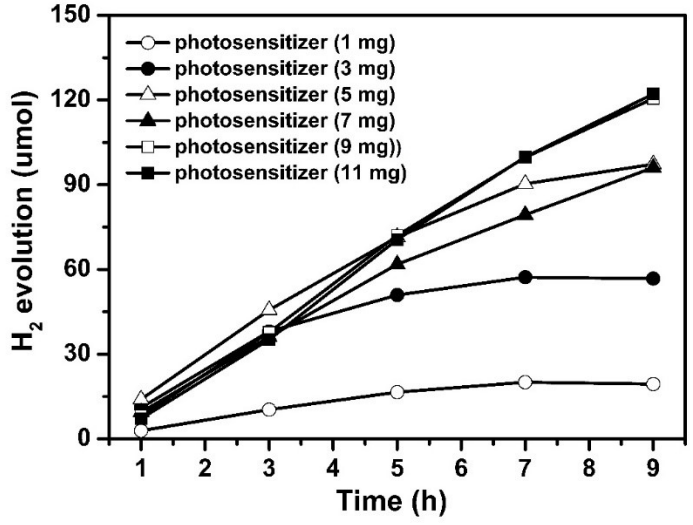

Figure S13. The effect of the different mass of photosensitizer on H_2 evolution. H_2 evolution condition: EtOH/H_2O (1:1) in the presence of 2 mg of CCMOF in 30 mL solution containing TEA (3 mL) under an inert atmosphere. The system was irradiated with visible light.

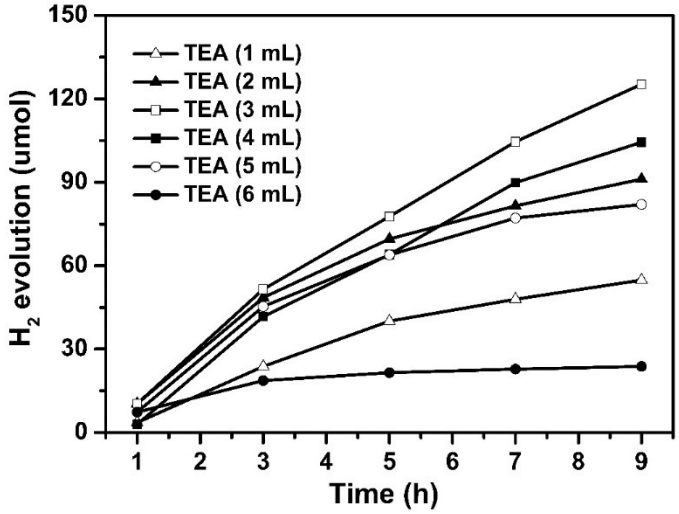

Figure S14. The effect of the volume of sacrificial agent on H_2 evolution. H_2 evolution condition: EtOH/H_2O (1:1) in the presence of 2 mg of CCMOF and 9 mg of fluorescein under an inert atmosphere. The system was irradiated with visible light.

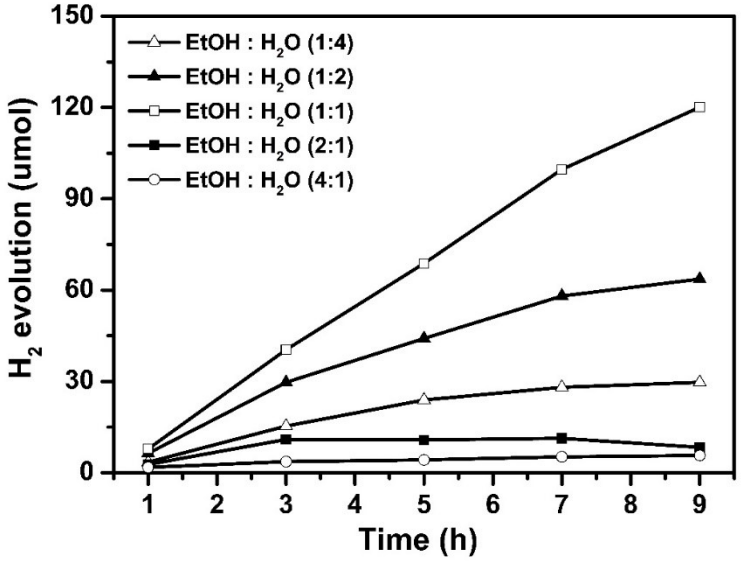

Figure S15. The effect of the ratio of the solvent on H_2 evolution. H_2 evolution condition: 2 mg of CCMOF in 30 mL solution containing TEA (3 mL) and 9 mg of fluorescein under an inert atmosphere. The system was irradiated with visible light.

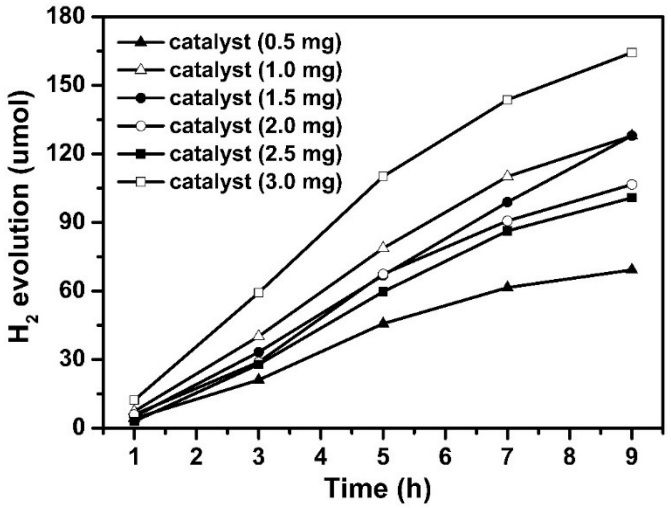

Figure S16. The effect of the different mass of catalysts on H_2 evolution. H_2 evolution condition: EtOH/H_2O (1:1) in the presence of 9 mg of fluorescein in 30 mL solution containing TEA (3 mL) under an inert atmosphere. The system was irradiated with visible light.

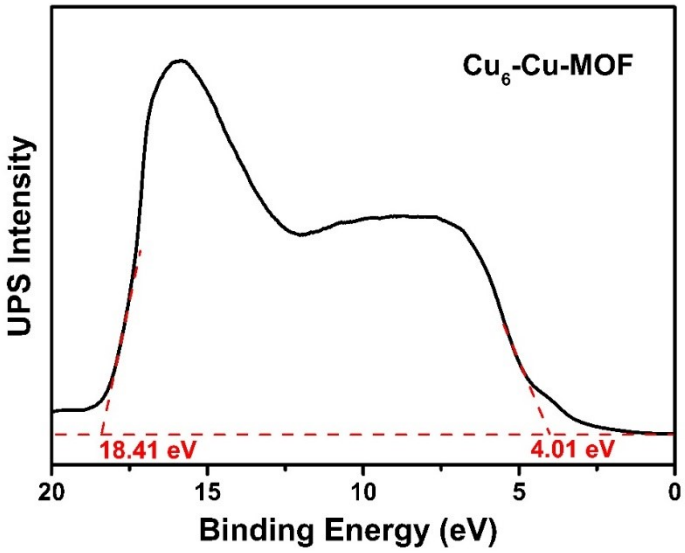

Figure S17. UPS spectrum of CCMOF.

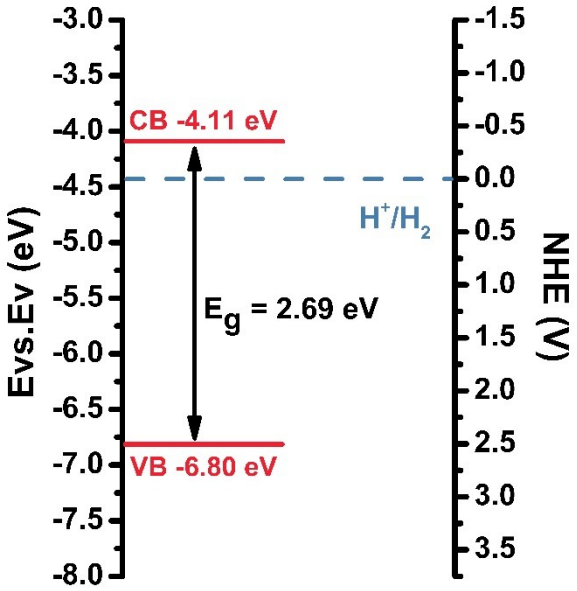

Figure S18. The band structure diagram of CCMOF.

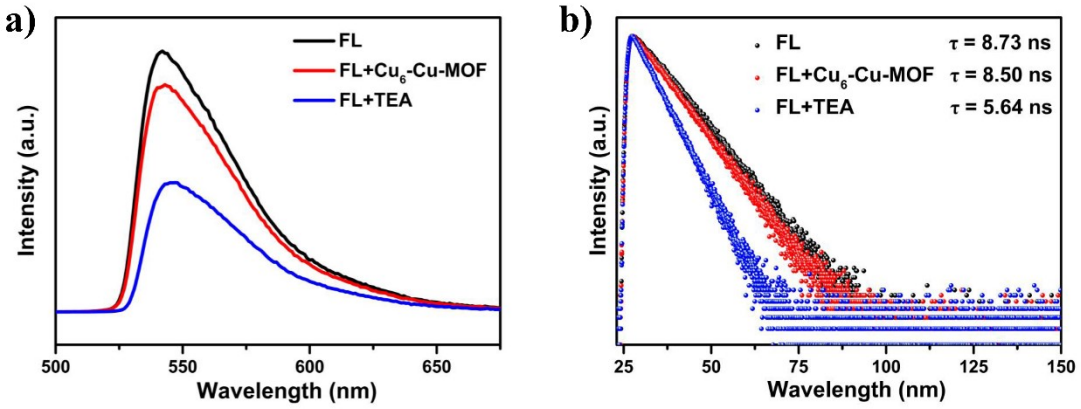

Figure. 19 (a) Fluorescent spectra of FL solution upon addition of TEA and CCMOF; (b) The corresponding TRPL lifetime decay curves.

Table S5 Photocatalytic activity of some typical MOF-based and MOF-derived catalysts for hydrogen production.

MOFs photocatalyst	Co-catalyst	Photosensitizer	Activity	Ref.
Pt@USTC-8(In)	Pt	No	340 μmol g^{-1} h^{-1}	5
Al-TCPP-0.1Pt	Pt	No	129 μmol g^{-1} h^{-1}	6
MIL-125-$(SCH_3)_2$	Pt	No	3814 μmol g^{-1} h^{-1}	7
MOF-253-Pt	Pt	No	100-200 μmol g^{-1} h^{-1}	8
Dy-MOF	Pt	No	21.53 μmol g^{-1} h^{-1}	9
ZSTU-1	Pt	No	1350 μmol g^{-1} h^{-1}	10
Pt/Ti-MOF-NH_2	Pt	No	3.3 μmol h^{-1}	11
$[Cu_4(DNP)(SCN)Cl_4]_n$	H_2PtCl_6	No	27.5 μmol g^{-1} h^{-1}	12
Pt@UiO-66-NH_2	Pt	No	257.38 μmol g^{-1} h^{-1}	13
Pt@UiO-66	Pt	Rhodamine B	116 μmol g^{-1} h^{-1}	14
Pd@UiO-66	Pd	Eosin Y	2280μmol g^{-1} h^{-1}	15
$Co_3(HL)_2 \cdot 4DMF \cdot 4H_2O$	No	$Ru(bpy)_3Cl_2$	1102 μmol g^{-1} h ^{1}	16
CdS@UiO-66	No	CdS	1725 μmol g^{-1} h^{-1}	17
$[Zr_6(\mu_3\text{-}O)_4(\mu_3\text{-}OH)_4(L1)_6](CO_2CF_3)_6$	No	$[(n\text{-}C_4H_9)_4N]_{10}[Ni_4(H_2O)_2(PW_9O_{34})_2]$	7.88 mmol g^{-1} h ^{1}	18
$[Ni_2(PymS)_4]n$	No	Fluorescein	6 μmol h^{-1}	19
Cu-RSH	No	Eosin Y	7.88 mmol g^{-1} h^{-1}	20
MET-Cu-D	No	Eosin Y	2582 μmol g^{-1} h^{-1}	21
$\{[Cu^{I}Cu^{II}{}_2(DCTP)_2]NO_3 \cdot 1.5DMF\}n$	H_2PtCl_6	No	32 μmol g^{-1} h^{-1}	22
$\{[Cu(HDSPTP)_2(H_2O)_3] \cdot 6H_2O\}_n$	No	No	5.77 μmol h^{-1}	23
Cu_6-Cu-MOF	**No**	**Fluorescein**	**14.22 mmol g^{-1} h^{-1}**	**This work**

References

1 G. M. Sheldrick, *Acta Cryst. A*, 2008, **64**, 112-122.

2 O. V. Dolomanov, L. J. Bourhis, R. J. Gildea, J. A. K. Howard and H. Puschmann, *J. Appl. Crystallogr.*, 2009, **42**, 339-341.

3 G. Sheldrick, *Acta Cryst. C*, 2015, **71**, 3-8.

4 W. Liu, Y. Fang, G. Z. Wei, S. J. Teat, K. Xiong, Z. Hu, W. P. Lustig and J. Li, *J. Am. Chem. Soc.*, 2015, **137**, 9400-9408.

5 F. Leng, H. Liu, M. Ding, Q.-P. Lin and H.-L. Jiang, *ACS Catal.*, 2018, **8**, 4583-4590.

6 X. Fang, Q. Shang, Y. Wang, L. Jiao, T. Yao, Y. Li, Q. Zhang, Y. Luo and H. L. Jiang, *Adv. Mater.*, 2018, **30**, 1705112.

7 S. Y. Han, D. L. Pan, H. Chen, X. B. Bu, Y. X. Gao, H. Gao, Y. Tian, G. S. Li, G. Wang, S. L. Cao, C. Q. Wan and G. C. Guo, *Angew. Chem. Int. Ed.*, 2018, **57**, 9864-9869.

8 T. Zhou, Y. Du, A. Borgna, J. Hong, Y. Wang, J. Han, W. Zhang and R. Xu, *Energy Environ. Sci.*, 2013, **6**, 3229-3234.

9 Q. Yu, H. Dong, X. Zhang, Y.-X. Zhu, J.-H. Wang, F.-M. Zhang and X.-J. Sun, *CrystEngComm*, 2018, **20**, 3228-3233.

10 C. Li, H. Xu, J. Gao, W. Du, L. Shangguan, X. Zhang, R.-B. Lin, H. Wu, W. Zhou, X. Liu, J. Yao and B. Chen, *J. Mater. Chem. A*, 2019, **7**, 11928-11933.

11 T. Toyao, M. Saito, Y. Horiuchi, K. Mochizuki, M. Iwata, H. Higashimura and M. Matsuoka, *Catal. Sci. Technol.*, 2013, **3**, 2092-2097.

12 L. Li, L. Huang, Z.-Y. Liu, X.-J. Zhao and E.-C. Yang, *Anorg. Allg. Chem.*, 2019, **645**, 623-630.

13 J.-D. Xiao, Q. Shang, Y. Xiong, Q. Zhang, Y. Luo, S.-H. Yu and H.-L. Jiang, *Angew. Chem. Int. Ed.*, 2016, **55**, 9389-9393.

14 D. Kim, D. R. Whang and S. Y. Park, *J. Am. Chem. Soc.*, 2016, **138**, 8698-8701.

15 Z. Jin and H. Yang, *Nanoscale Res. Lett.*, 2017, **12**, 539.

16 W.-M. Liao, J.-H. Zhang, Z. Wang, Y.-L. Lu, S.-Y. Yin, H.-P. Wang, Y.-N. Fan, M. Pan and C.-Y. Su, *Inorg. Chem.*, 2018, **57**, 11436-11442.

17 H.-Q. Xu, S. Yang, X. Ma, J. Huang and H.-L. Jiang, *ACS Catal.*, 2018, **8**, 11615-11621.

18 X.-J. Kong, Z. Lin, Z.-M. Zhang, T. Zhang and W. Lin, *Angew. Chem. Int. Ed.*, 2016, **55**, 6411-6416.

19 Y. Feng, C. Chen, Z. Liu, B. Fei, P. Lin, Q. Li, S. Sun and S. Du, *J. Mater. Chem. A*, 2015, **3**, 7163-7169.

20 X.-Y. Dong, M. Zhang, R.-B. Pei, Q. Wang, D.-H. Wei, S.-Q. Zang, Y.-T. Fan and T. C. W. Mak, *Angew. Chem. Int. Ed.*, 2016, **55**, 2073-2077.

21 Z.-D. Wang, Y. Zang, Z.-J. Liu, P. Peng, R. Wang and S.-Q. Zang, *Appl. Catal. B Environ.* , 2021, **288**, 119941.

22 Z.-L. Wu, C.-H. Wang, B. Zhao, J. Dong, F. Lu, W.-H. Wang, W.-C. Wang, G.-J. Wu, J.-Z. Cui and P. Cheng, *Angew. Chem. Int. Ed.*, 2016, **55**, 4938-4942.

23 T. Song, L. Zhang, P. Zhang, J. Zeng, T. Wang, A. Ali and H. Zeng, *J. Mater. Chem. A*, 2017, **5**, 6013-6018.